Supplementary Information

Cytotoxicity of nucleus-targeting fluorescent gold nanoclusters

Jing-Ya Zhao,[a] Ran Cui,[a] Zhi-Ling Zhang,[a] Mingxi Zhang,[b] Zhi-Xiong Xie[c] and Dai-Wen Pang *[a]

[a]*Key Laboratory of Analytical Chemistry for Biology and Medicine (Ministry of Education), College of Chemistry and Molecular Sciences, State Key Laboratory of Virology, and Wuhan Institute of Biotechnology, Wuhan University, Wuhan, 430072, P. R. China*

[b]*State Key Laboratory of Advanced Technology for Materials Synthesis and Processing, Wuhan University of Technology, Wuhan 430070, P. R. China*

[c]*College of Life Sciences, Wuhan University, Wuhan, 430072, P. R. China*

*Corresponding author. Tel.: +86 27 68756759; fax: +86 27 68754067.

E-mail address: dwpang@whu.edu.cn (D. W. Pang)

Figures

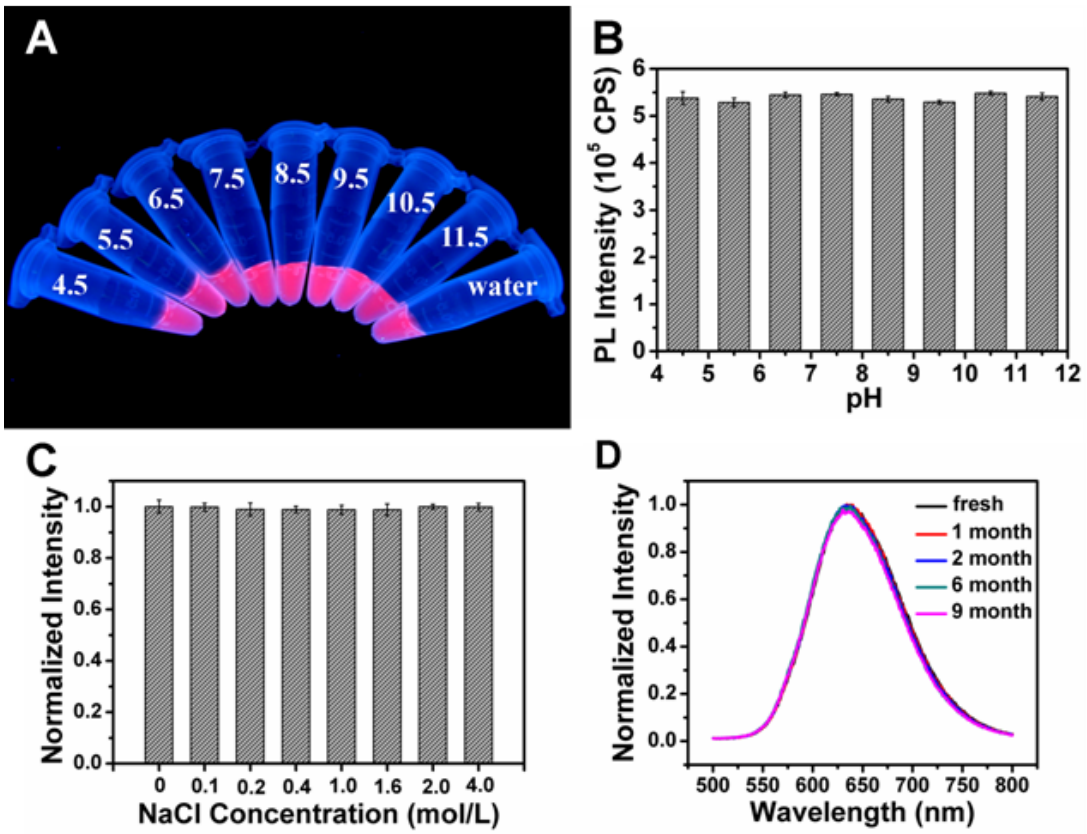

Fig. S1. Fluorescence photograph (A) and intensity (B) of Au_{25}NCs in BR buffer at pH value from 4.5 to 11.5. (C) Fluorescence intensity of Au_{25}NCs in aqueous solution with different concentration of NaCl. (D) Fluorescence spectra of Au_{25}NCs stored at 4 °C for different time.

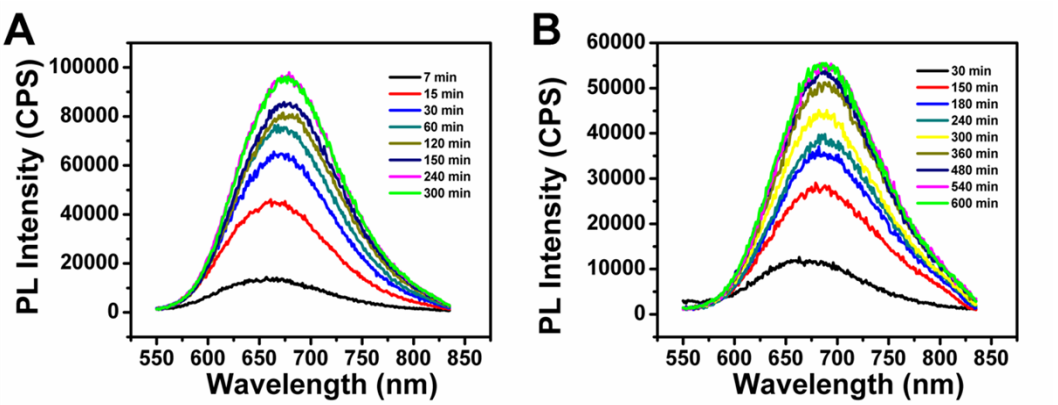

Fig. S2. Time evolution of the photoluminescence spectra for the preparation of fluorescent AuNCs by adopting Au(I) complex (A) and $HAuCl_4$ (B) as gold precursor.

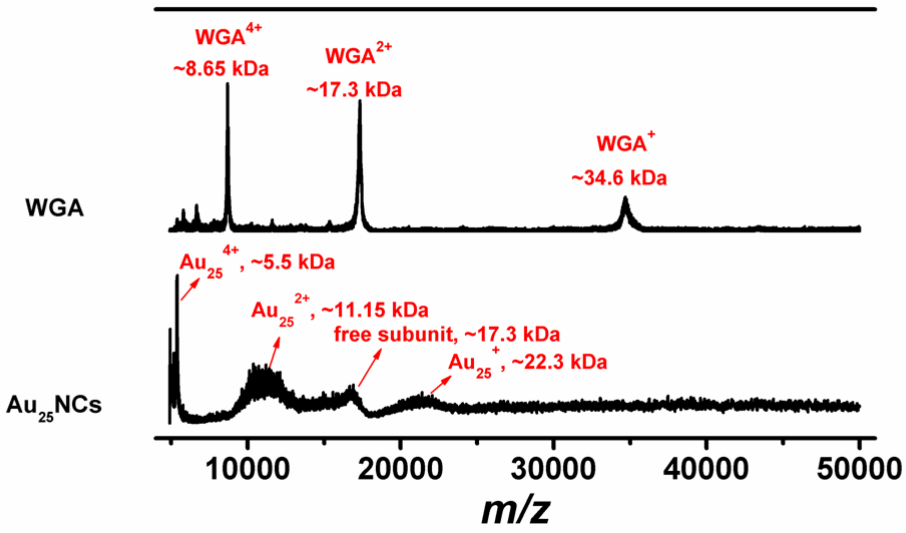

Fig. S3. MALDI-TOF mass spectra of WGA and Au_{25}NCs. The MALDI-TOF mass spectra were performed using matrixes of α-cyano-4-hydroxycinnamic acid in positive ion mode.

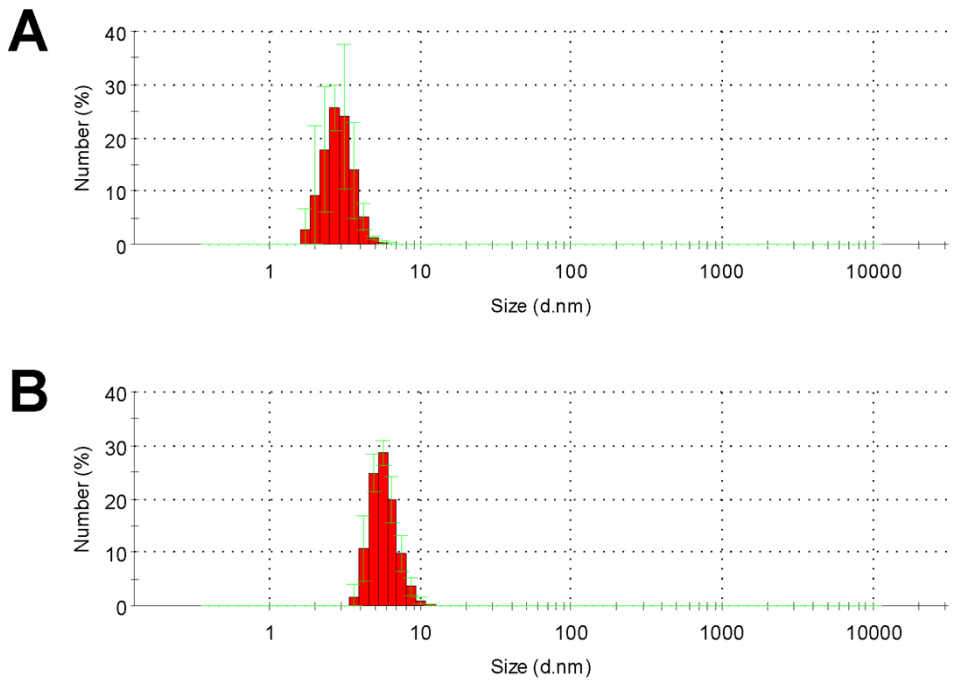

Fig. S4. Hydrodynamic sizes of Au_{25}NCs before (A) and after (B) conjugation with streptavidin.

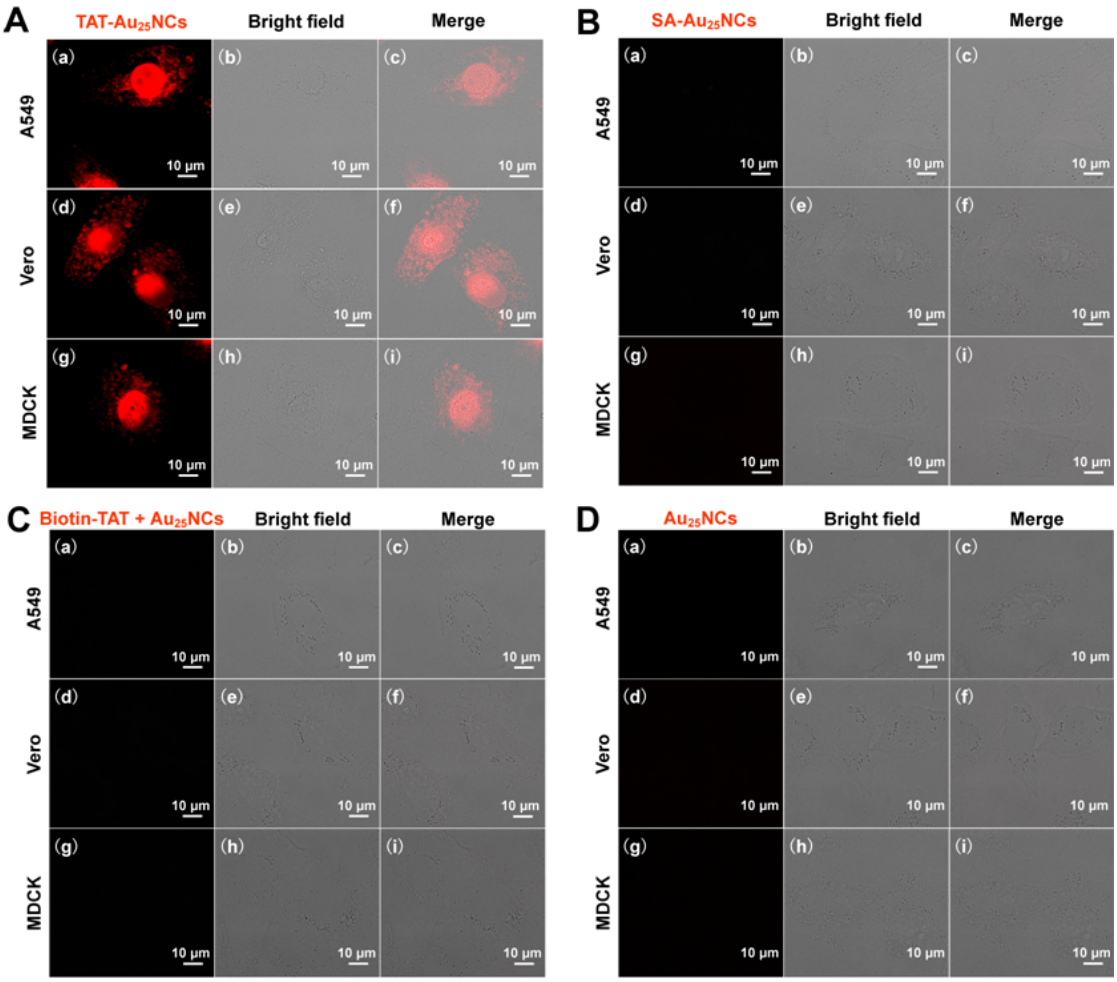

Fig. S5. Fluorescence microscopic images of A549 cells (a-c), Vero cells (d-f) and MDCK cells (g-i) treated with TAT-Au_{25}NCs (A), SA-Au_{25}NCs (B), a mixture of biotin-TAT and Au_{25}NCs (C) and Au_{25}NCs (D).

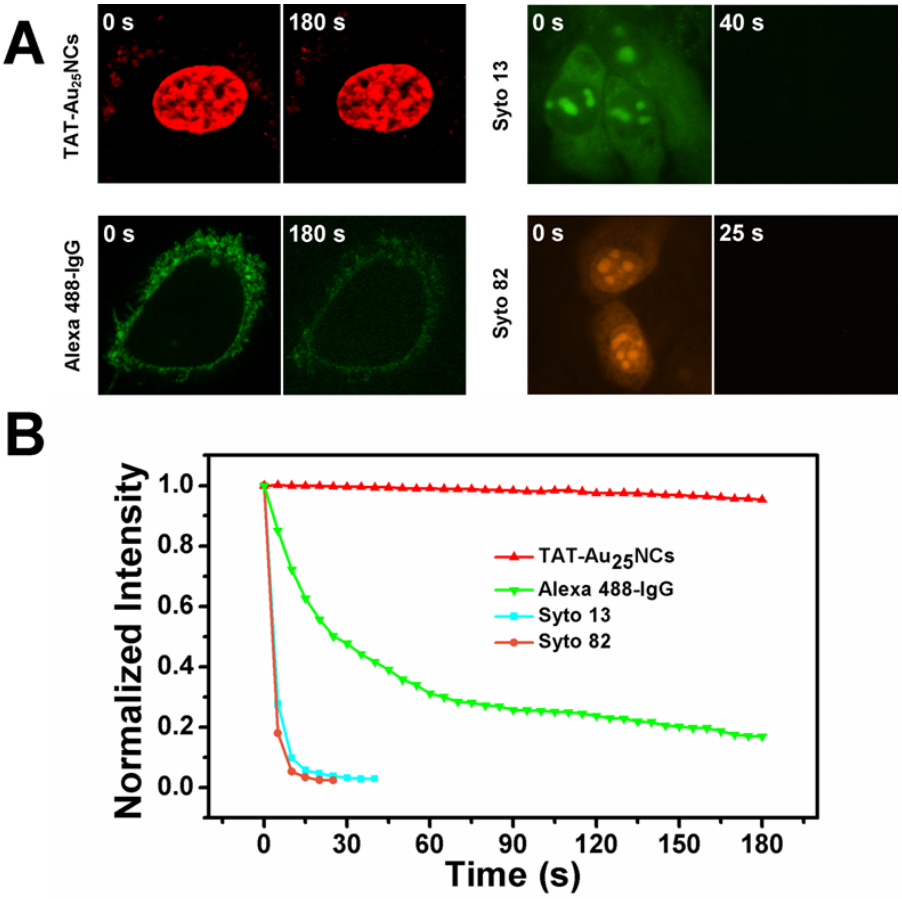

Fig. S6. (A) Photostability comparison between TAT-Au_{25}NCs and Alexa 488-IgG, Syto 13 and Syto82. TAT-Au_{25}NCs: Cal 27 cells were incubated with 2.4 μmol/L TAT-Au_{25}NCs for 1 h at 37 °C and then the cells were fixed by paraformaldehyde; Alexa 488-IgG: Paraformaldehyde-fixed and BSA-blocked Cal 27 cells were incubated sequentially with a mouse anti-epithelial-cell-adhesion-molecular antibody and Alexa 488 conjugated to goat anti-mouse immunoglobulin G (Alexa 488-IgG) for 1 h each; Syto 13: Cal 27 cells were incubated with 500 nM Syto 13 nucleic acid dye for 30 min at 37 °C and then the cells were fixed by paraformaldehyde; Syto 82: Cal 27 cells were incubated with 500 nM Syto 13 nucleic acid dye for 30 min at 37 °C and then the cells were fixed by paraformaldehyde. Then the specimens were continuously illuminated for 3 min with a 488 nm laser (laser energy 13 mW). Fluorescence images were acquired using an Andor Revolution XD laser confocal microscope at 5 s intervals. (B) Photostability curves of TAT-Au_{25}NCs, Alexa 488-IgG, Syto 13 nucleic acid dye and Syto 82 nucleic acid dye. Quantitative analysis of the changes in fluorescence intensities were performed by the ImageJ software.

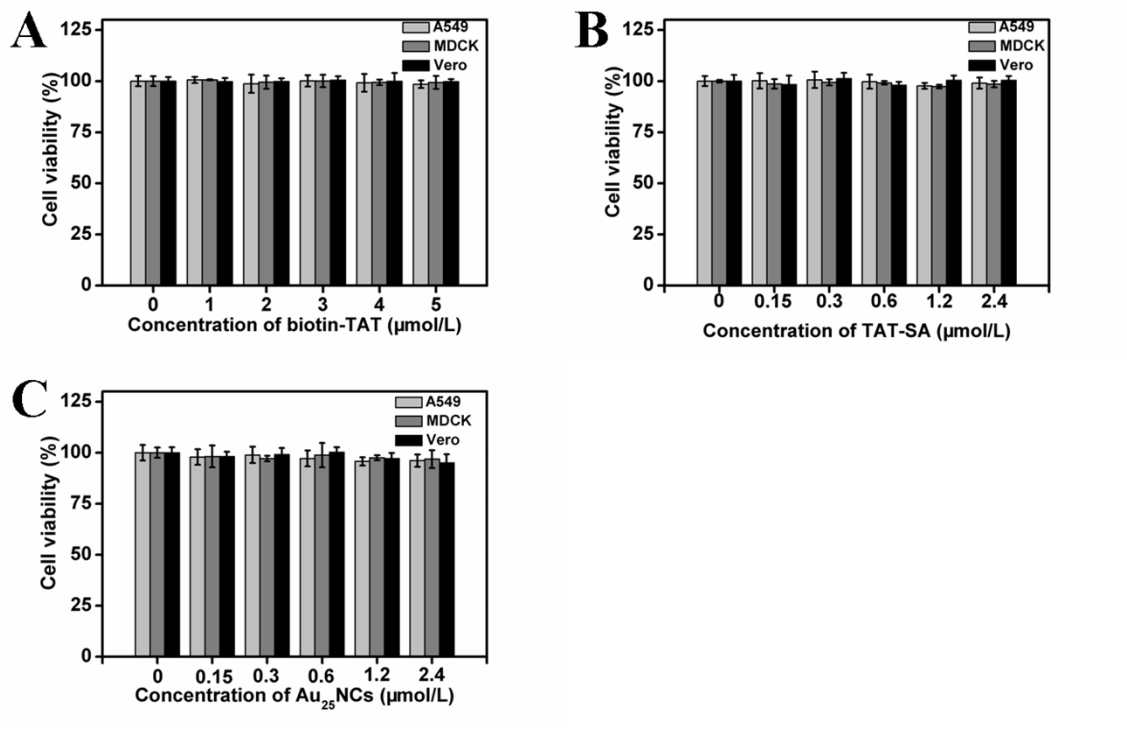

Fig. S7. MTT assay of A549 cells, MDCK cells and Vero cells treated with different concentrations of biotin-TAT (A), TAT-SA (B) and Au_{25}NCs(C) for 24 h.

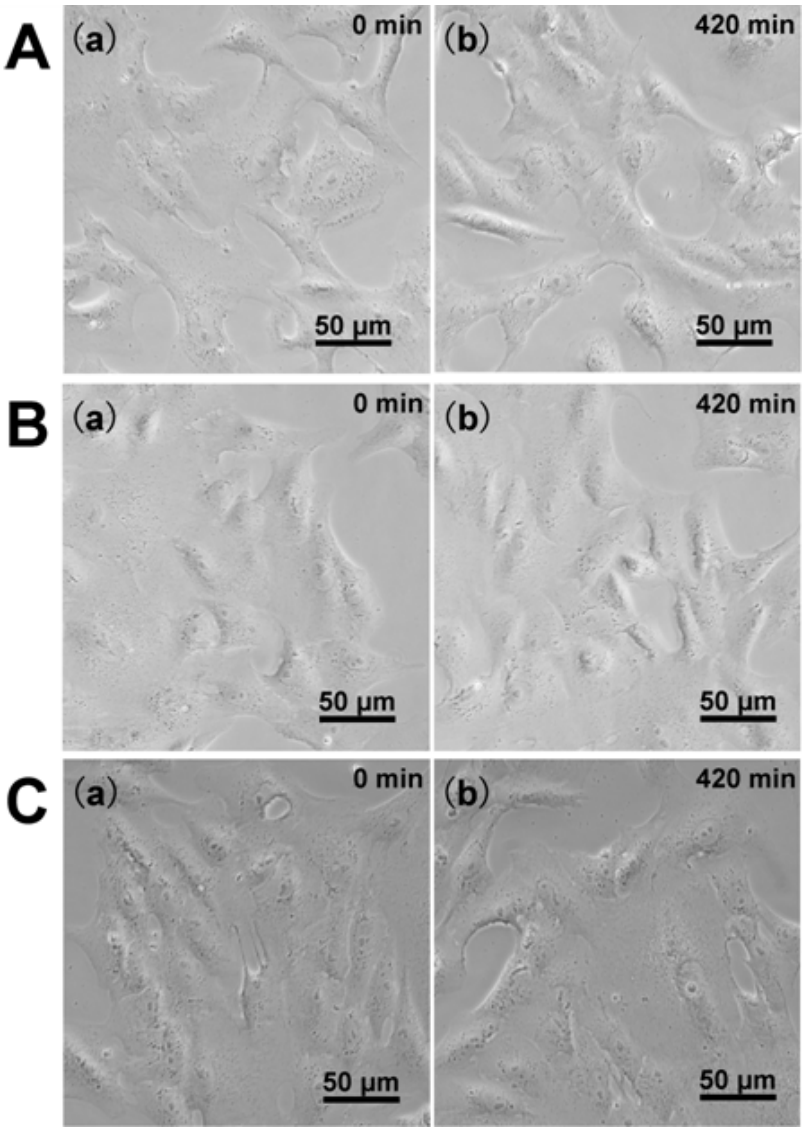

Fig. S8. Microscopic images of untreated (A), biotin-TAT treated (B) and TAT-SA treated (C) Vero cells at 0 min (a) and 420 min (b) post-treating. Vero cells were incubated with 4.8 μmol/L biotin-TAT (B) and 2.4 μmol/L TAT-SA (C) for 1 h and then were supplied with fresh medium and observed on the microscope.

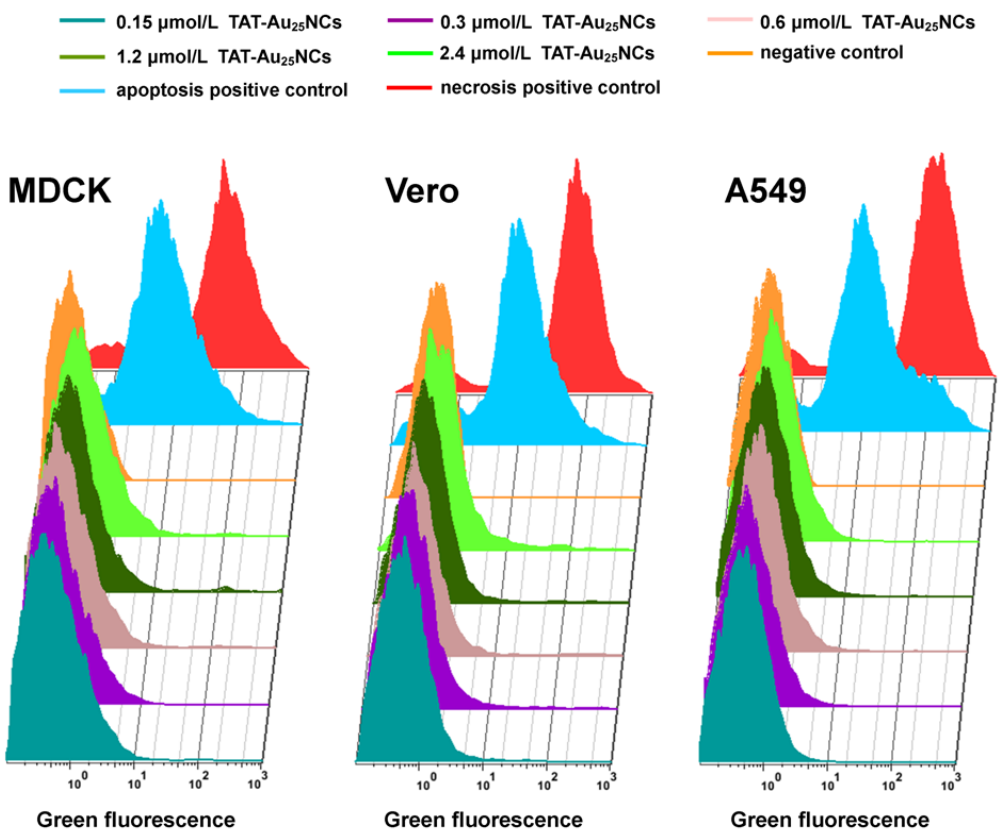

Fig. S9. Appoptosis assay on cells exposed to different concentrations of TAT-Au_{25}NCs for 2 h. Cells treated with 1 mM H_2O_2 and 0.1 μM actinomycin D were used as the necrosis positive control and apoptosis positive control, respectively.